

# A Loop-Opening Model for the Intrinsic Fracture Energy of Polymer Networks

Shu Wang, Chase M. Hartquist, Bolei Deng, and Xuanhe Zhao\*



Cite This: <https://doi.org/10.1021/acs.macromol.4c00308>



Read Online

ACCESS |



Metrics & More

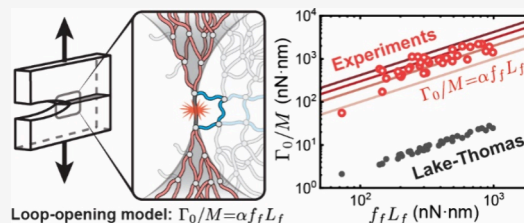


Article Recommendations



Supporting Information

**ABSTRACT:** We present a loop-opening model that accounts for the molecular details of the intrinsic fracture energy for fracturing polymer networks. This model includes not only the energy released from the scission of bridging chains but also the subsequent energy released from the network continuum. Scission of a bridging chain releases the cross-links and opens the corresponding topological loop. The released cross-links will be caught by the opened loop to reach a new force-balanced state. The amount of energy released from the network continuum is limited by the stretchability of the opened loop. Based on this loop-opening process, we suggest that the intrinsic fracture energy per broken chain approximately scales with the product of the fracture force and the contour length of the opened loop. This model predicts an intrinsic fracture energy that aligns well with various experimental data on the fracture of polymer networks.



## INTRODUCTION

Polymer networks are found in everyday items as diverse as automobile tires and hydrogels, but fracture events limit the life span of their service.<sup>1–3</sup> The connection between the fracture of polymer networks and their constituent polymer chains is unclear, hindering a deeper molecular understanding of their fracture behaviors. Lake and Thomas realized more than 50 years ago that the fracture energy of a polymer network is inherently linked to its polymer chains.<sup>4</sup> They defined the intrinsic fracture energy of a polymer network as the minimum energy needed to propagate a crack by creating a unit of new surface area and assumed that the intrinsic fracture energy depends solely on the breaking of elastically active polymer chains. The Lake–Thomas model predicts the intrinsic fracture energy  $\Gamma_0$  by multiplying the number of broken polymer chains per unit of new surface area  $M$  with the energy needed to break a chain at the crack tip  $U_{\text{chain}}$  (Figure 1a):

$$\Gamma_0 = MU_{\text{chain}} \quad (1)$$

The original Lake–Thomas model<sup>4</sup> further considers  $U_{\text{chain}} = NU_{\text{mon}}$  as the energy for rupturing a bridging chain (Figure 1a), where  $N$  is the number of repeating units and  $U_{\text{mon}}$  is the total bond dissociation energy per unit. This estimate has been widely used and provides fair predictions for the fracture energy of polymer networks. However, it has been shown to neglect certain physical and chemical feature of polymer chain scission. Recently, Wang et al.<sup>5</sup> calculated the single-chain energy  $U_{\text{chain}}$  as the area under the force–displacement curve up to the point where the chain fractures at the fracture force  $f_f$  and showed that  $U_{\text{chain}}$  is much lower than  $NU_{\text{mon}}$ . Wang et al. suggest that the reaction kinetics of chain scission dictate the

criterion for crack propagation.<sup>5</sup> With their estimation, the intrinsic fracture energy predicted by eq 1 underestimates various experimental results by 1–2 orders of magnitude (Table 1).

Extensive efforts have been made to explain why the Lake–Thomas model significantly underestimates the intrinsic fracture energy of polymer networks.<sup>6,9–11</sup> Several tree-like models<sup>10,11</sup> have been proposed to account for the energy released from unbroken chains connecting to a bridging chain when it breaks at  $f_f$  (Figure 1b). These models suggest that  $\Gamma_0/M$  should be equated with the energy stored in the tree-like structure rather than the single-chain energy. The tree-like models predict a higher intrinsic fracture energy per bridging chain, especially when considering infinite trees.<sup>11</sup> However, the concept of infinitely large trees does not realistically apply to actual polymer networks since real polymer networks consist of finite trees due to finite topological loops.<sup>12,13</sup>

Numerical simulations of lattice-like polymer network models have demonstrated that  $\Gamma_0/M$  is inherently much larger than  $U_{\text{chain}}$ .<sup>14,15</sup> The lattice-like polymer networks have well-defined topologies (Figure 1c), where each junction is freely joined with the same functionality. Each network edge exhibits the typical force–extension behavior of synthetic polymer chains with scission governed by the fracture force  $f_f$

**Received:** February 5, 2024

**Revised:** April 2, 2024

**Accepted:** June 7, 2024

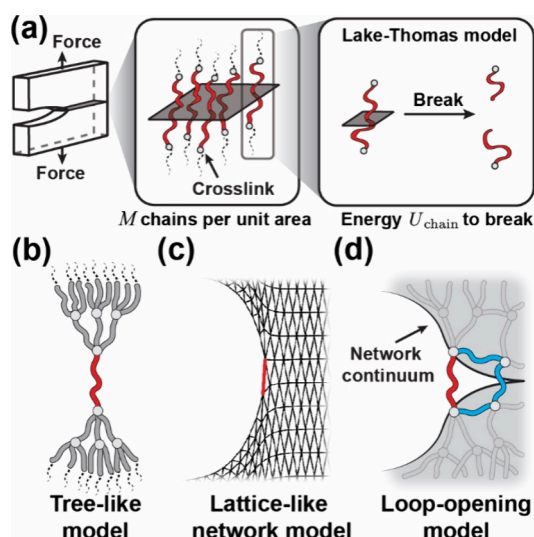


**Figure 1.** (a) Schematic illustration of various models for the intrinsic fracture energy of the polymer networks. The Lake–Thomas model only considers the energy released and dissipated in the bridging chains. (b) The tree-like model considers the energy released and dissipated in the network continuum as Caley tree structures. (c) The lattice-like network model is a numerical model that considers the energy released and dissipated in the network continuum, but it simplifies the networks to well-defined lattice structures. (d) The loop-opening model of polymer networks considers the opening of finite topological loops and the retraction of the network continuum after bridging chain scission. It considers both the energy released and dissipated in the network continuum.

**Table 1.** Comparison between  $\Gamma_0/M$  and Corresponding  $U_{\text{chain}}$  of End-Linked Poly(ethylene glycol) (PEG) Networks

	Wang et al. <sup>7</sup>	Lin et al. <sup>8</sup>	Akagi et al. <sup>6</sup>	Barney et al. <sup>9</sup>
$\Gamma_0/M^a$ (nN·nm)	430	872	351	528
$U_{\text{chain}}^b$ (nN·nm)	5.5	14.7	4.6	3.6
$\Gamma_0/MU_{\text{chain}}$	78	60	76	145

<sup>a</sup>Areal number density  $M$  is estimated based on the storage moduli of the networks. <sup>b</sup> $U_{\text{chain}}$  is estimated based on the data of storage moduli, single-molecule force spectroscopy experiments, and typical breaking forces of the backbone bonds. Detailed calculations can be found in the Supporting Information.

along the edge. The intrinsic fracture energies in these networks were measured using the “Rivlin–Thomas” method in the pure-shear geometry.<sup>1</sup> Comparisons between the simulated  $\Gamma_0$  and the predictions of the Lake–Thomas model (eq 1) revealed that the intrinsic fracture energy obtained by fracturing the network is significantly larger than  $MU_{\text{chain}}$ , consistent with the data in Table 1. The numerical simulations of the lattice-like polymer network models suggest that a substantial amount of energy is released and dissipated within the network continuum. While the lattice-like network unveils that the nonlocal energy dissipation in the network continuum significantly contributes to the intrinsic fracture energy, it is obviously an oversimplification (e.g., Figure 1c) for the topology of realistic polymer networks.

Here we propose a loop-opening model for the intrinsic fracture energy of polymer networks that accounts for both nonlocal energy dissipation in the network continuum and polymer network topology (Figure 1d). This model includes finite topological loops that open during crack propagation, unlike the infinite topological loops in the tree-like models.

The retraction of the network continuum (shaded in Figure 1d) balances with the unraveling of the loop (blue strands in Figure 1d), and the new force-balanced state is largely dictated by the stretchability of the opened loop. The loop-opening model provides a new relation for the intrinsic fracture energy of polymer networks

$$\frac{\Gamma_0}{M} = \alpha f_f L_f \quad (2)$$

where  $f_f$  and  $L_f$  are the critical force and length at the chain fracture and  $\alpha$  is a parameter proportional to the number of network chains in the opened loop. The physical meaning of  $\alpha$  is discussed in a later section on the loop-opening model; however, this explanation provides that the parameter  $\alpha$  is on the order of unity, suggesting that  $\Gamma_0/M$  is on the order of  $f_f L_f$  and is much larger than  $U_{\text{chain}}$ . Hence, the loop-opening model (eq 2) predicts the intrinsic fracture energy to be 1–2 orders of magnitude higher than the Lake–Thomas model (eq 1).

In the remainder of this article, we introduce the force–extension behavior of a single polymer chain and the corresponding network continuum. We then integrate the single-chain behavior with the network continuum to demonstrate our proposed loop-opening model and its new relation. At the end, we validate our model by comparing it to experimental data and discuss the differences between our model and other molecular fracture models of polymer networks.

## ■ SINGLE CHAIN AND NETWORK CONTINUUM

We begin with the force–extension behavior of single polymer chains.<sup>16,17</sup> Experiments have shown that the force–extension behaviors of common synthetic polymers align well with the modified freely jointed chain model (m-FJC)<sup>16,17</sup>

$$\frac{R(f)}{L} = \mathcal{L}\left(\frac{f}{f_s}\right) \left(1 + \frac{f}{f_e}\right) \quad (3)$$

where  $R$  is the end-to-end distance,  $f$  is the tension along the chain,  $L$  is the force-free contour length of the polymer, and  $\mathcal{L}(x) = \coth(x) - 1/x$  is the Langevin function. The characteristic entropic tension  $f_s = kT/b$  characterizes the initial linear entropic elasticity at the low force regime, where  $k$  is the Boltzmann constant,  $T$  is the absolute temperature, and  $b$  is the Kuhn length. The characteristic enthalpic tension  $f_e$  characterizes the linear enthalpic elasticity, which is typically 3 orders of magnitude larger than  $f_s$ . It describes the linear extension of the polymer backbone beyond force-free contour length  $L$ . Note that the polymer chain always breaks at  $f_f < f_e$ . The energy stored in a bridging chain at breakage  $U_{\text{chain}}$  is the area under the force–displacement curve up to the fracture point (Figure 2a).

When the crack propagates in a polymer network, a bridging chain is not directly connected to rigid boundaries. Instead, it is connected to an elastic network continuum that consists of other polymer chains (Figure 1d). We could simplify this by imagining that a polymer chain is connected to rigid boundaries through two networks (Figure 2b). To reach the fracture force of the bridging polymer chain  $f_f$ , the boundaries need to be displaced to  $L_{\text{boundary}}$ , which is much longer than the fracture length of bridging chain  $L_f$ . At the time the bridging chain ruptures, the network continues to store a significant amount of energy (gray area in Figure 2b). Additionally, the

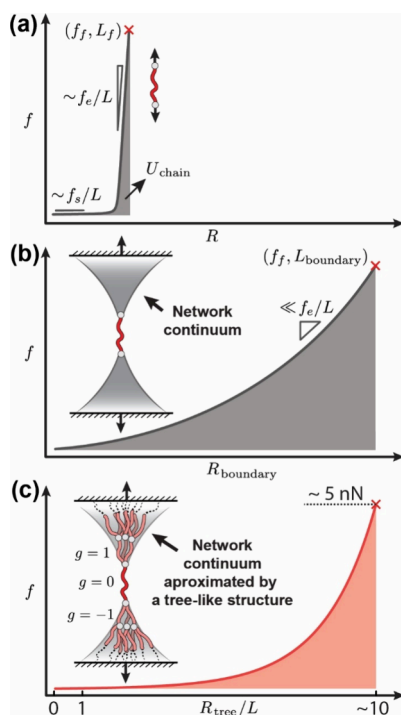


**Figure 2.** Schematic force–displacement curves for (a) a polymer chain and (b) a polymer chain connected to the rigid boundaries through elastic network continua. (c) A polymer chain connected to the rigid boundaries through tree-like structures as the elastic network continua. Typical polymer chains with  $f_f \approx 5 \text{ nN}$ ,  $f_s \approx 6 \text{ pN}$ , and  $f_e \approx 100 \text{ nN}$  (data from PEG chains<sup>17,19</sup>) provide the tree-like structure with  $z = 4$  and a rupture displacement about 10 times that of the bridging chain contour length  $L$ .

force–displacement curve for this whole combination (Figure 2b) is much more compliant than that of the single bridging chain at high forces. Because the load in the network continua is shared by many polymer chains in the direction of deformation, allowing the network continua to act like more compliant springs that store significant amounts of energy.

As an example, we can approximate the network continua as two Cayley trees connected to each end of the bridging chain, comprising identical polymer chains and cross-links (structures shown in Figure 2c). The trees' roots are linked to rigid boundaries. As the rigid boundaries separate, the tree-like structure deforms and stores elastic energy. With identical chains, the tensions and end-to-end displacements of all polymer chains in the same generation of the tree-like structure (Figure 2c) are almost the same. The tension of the bridging chain ( $g = 0$  in Figure 2c) equals the sum of the tensions of all chains in one generation of the tree-like structure. Therefore, the tension of a polymer chain in the  $g$ th generation of the tree-like structure is  $f/(z - 1)^{|g|}$ , where  $z$  is the functionality of cross-links.<sup>18</sup> Applying eq 3 to a tree-like structure, the force–displacement relationship of a tree-like structure can be expressed as<sup>11</sup>

$$R_{\text{tree}}(f) = \sum_g R \left( \frac{f}{(z - 1)^{|g|}} \right) = L \sum_g \mathcal{L} \left( \frac{f/(z - 1)^{|g|}}{f_s} \right) \times \left( 1 + \frac{f/(z - 1)^{|g|}}{f_e} \right) \quad (4)$$

where  $R_{\text{tree}}$  is the displacement of the boundary that the trees' roots are connected with,  $f$  is the tension on the bridging chain in  $g = 0$  (or the combined tension in a generation), and  $L$  is the force-free contour length of the network chains. A typical force–displacement curve obtained by eq 4 is shown in Figure 2c. Compared to a single chain, the tree-like structure deforms compliantly at high forces, extends much further, and stores more energy before the bridging chain ruptures. Although the scheme demonstrated here does not fully mirror the scenario of the bridging chain at the crack tip, this approximation qualitatively captures two key features: (1) the bridging chain at  $g = 0$  has the highest tension (analogous to stress–concentration at the crack tip of loaded notched polymer networks); (2) the network continua stores a lot of energy at the moment the bridging chain ruptures.

## LOOP-OPENING MODEL

Real polymer networks consist of finite topological loops.<sup>12,13,20</sup> The scission of a bridging chain leads to the opening of the corresponding loop. Consider a defect-free notched network composed of identical polymer chains (e.g., no dangling chains and first- or second-order loops). At the crack tip, we may consider that the network continua (shaded in Figure 3a) connect the bridging chain (dark gray in Figure 3a) to the distant boundaries, with a topological loop (blue) situated ahead of the bridging chain (dark gray). When the bridging chain is quasi-statically loaded to the fracture force  $f_f$ , the displacement of the two cross-links on the bridging chain  $R$  approaches the fracture displacement  $L_f$  (transitioning from state 1 to state 2 in Figure 3a). Throughout this process, the restoring force along the bridging chain can be represented by the m-FJC model (gray curve in Figure 3c). Meanwhile, the network continues to store elastic energy as well. When the bridging chain fractures, its two cross-links are left highly unbalanced due to the force  $f_f$  exerted by the elastic network continua (state 2 in Figure 3a). These cross-links then seek a new force-balanced state (state 3, Figure 3a). While the process from state 2 to state 3 is complex, we can still estimate the energy released.

Approximating the elastic network continua as the imaginary tree-like structures without the loss of generality (red chains in Figures 2c and 3a), we then decompose the process from state 2 to state 3 in Figure 3a into two components: the retraction of the elastic network continua (red tree-like structures in Figure 3b) and the extension of the opened loop (blue in Figure 3b). We may track these contributions by monitoring the imaginary forces required to quasi-statically unload the elastic network continuum, denoted as  $f_{\text{tree}}$  (eq S5 in the Supporting Information), and the imaginary force that is required to quasi-statically load the opened loop, denoted as  $f_{\text{loop}}$ . Note that  $f_{\text{loop}}$  is the imaginary force exerted on the cross-links; it does not imply the tensions are the same on the chains within the opened loop. These two forces are schematically plotted as functions of junction displacement in Figure 3c in red and blue, respectively. The former is much larger than the latter at state 2 ( $f_{\text{tree}} \gg f_{\text{loop}}$ ), but they counterbalance at state 3 ( $f_{\text{tree}} = f_{\text{loop}}$ ). In this assumed quasi-static unloading process, the energy released from state 2 to state 3 is  $U_{\text{release}}$  (red shaded area in Figure 3c), and the cross-links are displaced from  $L_f$  to approximately  $(n_{\text{loop}} - 1)L_f$  (Figure 3c), where  $n_{\text{loop}}$  is the number of polymer chains within the loop.

The energy released from state 2 to state 3 is eventually dissipated in the polymer network (e.g., viscous dissipation),



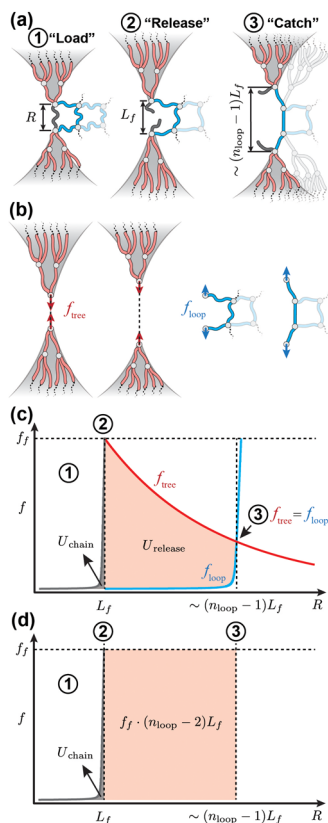


**Figure 3.** (a) Schematic illustration of the loop-opening model that consists of a three-step process: load, release, and then catch. State 2 is the moment when the bridging chain just breaks, leaving the network continua unstable. State 3 is the moment when the cross-links of the broken bridging chain reach a new force-balanced condition. (b) From state 2 to state 3, we decompose this process into two components: the retraction of the network continua (red trees) and the extension of the opened loop (blue chains). (c) The imaginary force that quasi-statically unloads the tree is shown in red, and the imaginary force that quasi-statically loads the opened loop is shown in blue. The difference gives the energy released in this process as  $U_{\text{release}}$ . (d) Direct comparison between the single-chain energy  $U_{\text{chain}}$  considered by the Lake–Thomas model and the energy  $f_f(n_{\text{loop}} - 2)L_f$  considered in the semiquantitative loop-opening model.

which contributes to the measured intrinsic fracture energy of the polymer network. Therefore, the loop-opening model predicts  $\Gamma_0/M \approx U_{\text{chain}} + U_{\text{release}} \approx U_{\text{release}}$  as  $U_{\text{release}} \gg U_{\text{chain}}$ . This energy  $U_{\text{release}}$  depends on the retraction behavior of the elastic network continuum (red curve) and the stretchability of the opened loop (blue curve).

Although we use the tree-like structures to approximate the network continua, it should be noted that the loop-opening model does not depend on the tree-like structures for the elastic network continua. Instead, any constitutive models that can characterize the generic features of the elastic network continuum (Figure 2b) are applicable to the loop-opening model. Additionally, the opened loop should balance the retraction of the network continuum, and its stretchability determines a limit for the retraction (Figure 3b,c). Therefore, rather than deriving an analytical solution for  $U_{\text{release}}$ , we propose a semiquantitative argument that  $U_{\text{release}}$  is proportional to  $f_f(n_{\text{loop}} - 2)L_f$  (Figure 3d). This represents the area of the rectangle between states 2 and 3 in Figure 3d, with  $(n_{\text{loop}} - 2)L_f$  as the displacement of two cross-links from state 2 to state

3 and  $f_f$  as the typical force scale during this process. Based on the loop-opening model, we can thus formulate a new relation for the intrinsic fracture energy of polymer networks

$$\frac{\Gamma_0}{M} = \alpha f_f L_f \approx (n_{\text{loop}} - 2) f_f L_f \quad (5)$$

where  $n_{\text{loop}}$  is the average number of network chains within the loop. The parameter  $\alpha$  is directly correlated to the average topological loop size  $n_{\text{loop}}$  in polymer networks. As we consider defect-free networks, all the loops have  $n_{\text{loop}} \geq 3$ , and the parameter  $\alpha \approx n_{\text{loop}} - 2 \geq 1$ . This suggests that the fracture energy per chain  $\Gamma_0/M$  is on the order of  $f_f L_f$ , which is much larger than the  $U_{\text{chain}}$  predicted by the Lake–Thomas model.

## COMPARISON WITH EXPERIMENTAL RESULTS

We next validated the loop-opening model by comparing its prediction of the intrinsic fracture energy with experimental results. The experiments were carried out by various groups using end-linked poly(ethylene glycol) (PEG) networks. The networks were synthesized through different end-linking strategies, including the end-linking of two different tetra-arm PEG macromers ( $A_4 + B_4$ ) by Akagi et al. and Lin et al., the end-linking of a tetra-arm PEG macromer with bifunctional small-molecule linkers ( $A_4 + B_2$ ) by Wang et al., and the end-linking of linear PEG with tetrafunctional small-molecule cross-linkers ( $A_2 + B_4$ ) by Barney et al. and Arora et al.<sup>7–9,21,22</sup> The gels were prepared under semidilute conditions and well below the entanglement concentration to avoid trapped entanglements. The moduli therefore correspond directly to the contributions of the elastically active chains. The moduli of the gels have been confirmed to be reasonably consistent with the phantom network model<sup>18</sup> and the real elastic network theory model.<sup>23</sup> Therefore, information about the elastically active chains, such as the areal number density  $M$  and the single-chain energy  $U_{\text{chain}}$ , can be extracted from the moduli of these gels. Detailed calculations can be found in the Supporting Information. The experimental results of  $\Gamma_0/M$  from various groups are plotted against  $f_f L_f$  in Figure 4 with red circles. The loop-opening model with different parameter  $\alpha$

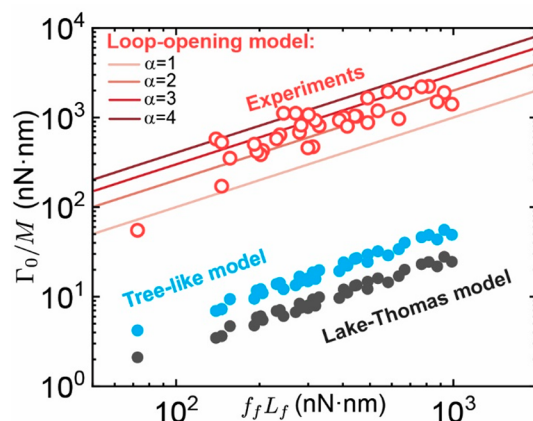


**Figure 4.** Plot of different fracture energy per chain  $\Gamma_0/M$  against the corresponding  $f_f L_f$ . Red solid lines depict the equation  $\Gamma_0/M = \alpha f_f L_f$  with  $\alpha = 1, 2, 3, 4$ . Red circles are  $\Gamma_0/M$  values estimated from experimental data of end-linked PEG gels. Black dots are  $\Gamma_0/M = U_{\text{chain}}$  based on the Lake–Thomas model. Blue dots are  $\Gamma_0/M \approx [z/(z - 2)]U_{\text{chain}} = 2U_{\text{chain}}$  based on the tree-like model<sup>10,11</sup> with functionality  $z = 4$ , assuming small loops.<sup>12,13</sup>

(solid red lines in Figure 4) is plotted alongside. The model and experimental data align well, and both significantly exceed the predictions of the Lake–Thomas model (eq 5 and black dots in Figure 4) and the tree-like model (blue dots in Figure 4). Note that the tree-like model depicted in Figure 4 involves small tree-like structures, which mainly consider the energetic elasticity of the network chains.<sup>10,11</sup> The average loop size limits the generations of tree-like structures.<sup>11</sup> Since the end-linked PEG gels presented in Figure 4 are expected to possess small topological loops,<sup>13</sup> we suppose the tree-like structures should be small.

In Figure 4, the Lake–Thomas model and the tree-like model show the same scaling relation with the loop-opening model and the experimental results, but the Lake–Thomas model and the tree-like model underestimate the experimental results by at least an order of magnitude. The loop-opening model (eqs 2 and 5) provides more quantitative estimates for the experimental data because it considers the energy release from the network continuum. The intrinsic fracture energy per broken chain  $\Gamma_0/M$  is predicted to be on the order of  $f_f L_f$  as mentioned before, since the parameter  $\alpha$  is on the order of unity. Most of the experimental data align closely with the loop-opening model with parameter  $\alpha = 2-4$ . Given that  $\alpha \approx n_{\text{loop}} - 2$ , this  $\alpha$  range implies that the average loop size,  $n_{\text{loop}}$ , in these end-linked PEG gels is approximately 4–6. This relatively small average loop size is to be expected for networks prepared just above overlap conditions<sup>12,13</sup> and aligns well with simulations of end-linked networks.<sup>20</sup> Recall that Lake and Thomas originally proposed  $\Gamma_0/M = NU_{\text{mon}}$ . Although this assumption was shown to neglect some chemical and physical features of chain scission, a detailed comparison between this assumption and the loop-opening model can be found in the Supporting Information.

## DISCUSSION

Several points regarding the loop-opening model are noteworthy. First, various models for the intrinsic fracture energy of polymer networks (Figure 1) assume different length scales for energy dissipation. The Lake–Thomas model considers only the energy dissipated in the bridging chain. The tree-like model considers the energy that can be dissipated in a tree-like structure. This involves the contribution from unbroken chains, but it still considers the energy to be dissipated below the scale of topological loops, as the tree-like structure only exists within the scale of such loops.<sup>12,13</sup> Numerical simulations of the lattice-like network model reveal the energy can be released and dissipated much beyond the scale of topological loops.<sup>14,15</sup> Albeit oversimplification, it leads to the physical picture developed in the loop-opening model, which considers the energy released and dissipated from both the network continuum and the broken bridging chain.

Second, for polymer networks with the same chemistry, the loop-opening model (eq 5) gives

$$\frac{\Gamma_0}{M} \sim N \quad (6)$$

since the fracture force  $f_f$  remains constant with variations in fracture chain length  $L_f \sim N$ , where  $N$  is the number of Kuhn segments of the network chains between cross-links. This mirrors the scaling behavior of the Lake–Thomas model (eq 1) since  $U_{\text{chain}} \sim N$ . This scaling law has been verified by many experiments.<sup>6</sup> Although both models follow the same scaling relation with respect to  $N$ , the loop-opening model provides

more quantitative estimates for the experimental results, which give values approximately 2 orders of magnitude larger than those predicted by the Lake–Thomas model (Figure 4).

Third, although the loop-opening model can provide good estimates for the intrinsic fracture energies of end-linked gels in which the loops are not heavily overlapped, it may not be suitable for polymer networks prepared under highly overlapped conditions.<sup>12,24</sup> This limitation arises because the model assumes that the loops can be fully opened. Overlapped topological loops and entanglements of network chains might impede complete loop opening. In such a scenario, the extent to which unbalanced junctions can retract after a bridging chain breaks remains a quantity of interest, although this retraction might not be directly dictated by the contour length of the opened loops. The factors controlling the retraction of junctions at the crack tip in highly overlapped polymer networks remain an open question.

Fourth, the loop-opening model for polymer networks shares some similarities with the lattice trapping model in crystal fracture. Both models focus on the local stress and load at the crack tip, extending beyond the thermodynamic limit of the Griffith theory<sup>25</sup> based on the bond dissociation energy. The former is pronounced in polymer networks according to Table 1 and Figure 4, while the latter is almost experimentally inaccessible in crystals due to thermal fluctuation. For more details on the lattice trapping model, readers are referred to the works of Thomson et al.,<sup>26</sup> Curtin,<sup>27</sup> and Marder.<sup>28</sup>

## CONCLUSION

The loop-opening model introduced in this study captures the intrinsic fracture energy of polymer networks by focusing on the energy released from the network continuum. The energy released per broken chain,  $\Gamma_0/M$ , is governed by the stretchability of polymer chains within the opened loop. Without further assumption of the constitutive law of the network continuum, this leads to a new relation,  $\Gamma_0/M = \alpha f_f L_f$  for polymer network fracture, which aligns well with experimental data from end-linked PEG gels. The model suggests that the intrinsic fracture energy of a polymer network stems from contributions at both the single-chain level and the network-continuum level. Moreover, the loop-opening model suggests that by either shielding the bridging chain from the fracture force or increasing its cross-links' maximum displacement before breaking the next chain (e.g., through larger topological loops) could enhance the fracture energy, resulting in tougher and more resilient polymeric materials. Coupled with continuous advancements in polymer characterization technology and precise chemical control of the force-coupled reactivities,<sup>7,29,30</sup> the topologies of polymer networks,<sup>31,32</sup> and chain conformations,<sup>33</sup> our model could offer deeper insights into the interplay between network fracture and the mechanics of individual chains, thereby paving the way for the design of more robust polymeric materials.

## ASSOCIATED CONTENT

### Supporting Information

The Supporting Information is available free of charge at <https://pubs.acs.org/doi/10.1021/acs.macromol.4c00308>.

Summary of the Lake–Thomas model and the loop-opening model; analysis of the experimental data in Table 1 and Figure 4; dependence of force–displacement on the retraction of tree-like structures (PDF)

## AUTHOR INFORMATION

### Corresponding Author

Xuanhe Zhao – Department of Mechanical Engineering and Department of Civil and Environment Engineering, Massachusetts Institute of Technology, Cambridge, Massachusetts 02139, United States; [orcid.org/0000-0001-5387-6186](https://orcid.org/0000-0001-5387-6186); Email: [zhaox@mit.edu](mailto:zhaox@mit.edu)

### Authors

Shu Wang – Department of Mechanical Engineering, Massachusetts Institute of Technology, Cambridge, Massachusetts 02139, United States; [orcid.org/0000-0001-7638-327X](https://orcid.org/0000-0001-7638-327X)

Chase M. Hartquist – Department of Mechanical Engineering, Massachusetts Institute of Technology, Cambridge, Massachusetts 02139, United States; [orcid.org/0000-0001-5273-4186](https://orcid.org/0000-0001-5273-4186)

Bolei Deng – Department of Mechanical Engineering, Massachusetts Institute of Technology, Cambridge, Massachusetts 02139, United States

Complete contact information is available at:  
<https://pubs.acs.org/10.1021/acs.macromol.4c00308>

### Author Contributions

S.W., C.M.H., and B.D. are co-first authors. The manuscript was written through contributions of all authors. All authors have given approval to the final version of the manuscript.

### Funding

This work is supported in part by the National Institutes of Health (Grants No. 1R01HL153857-01 and No. 1R01HL167947-01), the National Science Foundation (Grant No. EFMA-1935291), and Department of Defense Congressionally Directed Medical Research Programs (Grant No. PR200524P1).

### Notes

The authors declare no competing financial interest.

## ACKNOWLEDGMENTS

The authors thank W. A. Curtin for helpful discussions.

## REFERENCES

- (1) Rivlin, R. S.; Thomas, A. G. Rupture of Rubber. I. Characteristic Energy for Tearing. *J. Polym. Sci.* **1953**, *10* (3), 291–318.
- (2) Lake, G. J.; Lindley, P. B. The Mechanical Fatigue Limit for Rubber. *J. Appl. Polym. Sci.* **1965**, *9* (4), 1233–1251.
- (3) Bai, R.; Yang, J.; Suo, Z. Fatigue of Hydrogels. *Eur. J. Mech. A/Solids* **2019**, *74*, 337–370.
- (4) Lake, G. J.; Thomas, A. G. The Strength of Highly Elastic Materials. *Proc. R. Soc. London, Ser. A Math. Phys. Sci.* **1967**, *300* (1460), 108–119.
- (5) Wang, S.; Panyukov, S.; Rubinstein, M.; Craig, S. L. Quantitative Adjustment to the Molecular Energy Parameter in the Lake-Thomas Theory of Polymer Fracture Energy. *Macromolecules* **2019**, *52* (7), 2772–2777.
- (6) Akagi, Y.; Sakurai, H.; Gong, J. P.; Chung, U. I.; Sakai, T. Fracture Energy of Polymer Gels with Controlled Network Structures. *J. Chem. Phys.* **2013**, *139* (14), 144905.
- (7) Wang, S.; Beech, H. K.; Bowser, B. H.; Kouznetsova, T. B.; Olsen, B. D.; Rubinstein, M.; Craig, S. L. Mechanism Dictates Mechanics: A Molecular Substituent Effect in the Macroscopic Fracture of a Covalent Polymer Network. *J. Am. Chem. Soc.* **2021**, *143* (10), 3714–3718.
- (8) Lin, S.; Ni, J.; Zheng, D.; Zhao, X. Fracture and Fatigue of Ideal Polymer Networks. *Extrem. Mech. Lett.* **2021**, *48*, 101399.
- (9) Barney, C. W.; Ye, Z.; Sacligil, I.; McLeod, K. R.; Zhang, H.; Tew, G. N.; Riggleman, R. A.; Crosby, A. J. Fracture of Model End-Linked Networks. *Proc. Natl. Acad. Sci. U. S. A.* **2022**, *119* (7), 2–7.
- (10) Lin, S.; Zhao, X. Fracture of Polymer Networks with Diverse Topological Defects. *Phys. Rev. E* **2020**, *102* (5), 052503.
- (11) Wang, S.; Panyukov, S.; Craig, S. L.; Rubinstein, M. Contribution of Unbroken Strands to the Fracture of Polymer Networks. *Macromolecules* **2023**, *56* (6), 2309–2318.
- (12) Cai, L. H.; Panyukov, S.; Rubinstein, M. Hopping Diffusion of Nanoparticles in Polymer Matrices. *Macromolecules* **2015**, *48* (3), 847–862.
- (13) Panyukov, S. Loops in Polymer Networks. *Macromolecules* **2019**, *52*, 4145–4153.
- (14) Deng, B.; Wang, S.; Hartquist, C.; Zhao, X. Nonlocal Intrinsic Fracture Energy of Polymerlike Networks. *Phys. Rev. Lett.* **2023**, *131* (22), 228102.
- (15) Hartquist, C.; Wang, S.; Cui, Q.; Matusik, W.; Deng, B.; Zhao, X. A Universal Scaling Law for Intrinsic Fracture Energy of Networks. *arXiv Prepr.* **2024**, arXiv:2401.
- (16) Smith, S. B.; Cui, Y.; Bustamante, C. Overstretching B-DNA: The Elastic Response of Individual Double-Stranded and Single-Stranded DNA Molecules. *Science* **1996**, *271* (9), 795–799.
- (17) Oesterhelt, F.; Rief, M.; Gaub, H. E. Single Molecule Force Spectroscopy by AFM Indicates Helical Structure of Poly(Ethylene Glycol) in Water. *New J. Phys.* **1999**, *1*, 6.
- (18) James, H. M.; Guth, E. Theory of the Elastic Properties of Rubber. *J. Chem. Phys.* **1943**, *11* (10), 455–481.
- (19) Beyer, M. K. The Mechanical Strength of a Covalent Bond Calculated by Density Functional Theory. *J. Chem. Phys.* **2000**, *112* (17), 7307–7312.
- (20) Michalke, W.; Lang, M.; Kreitmeier, S.; Görnitz, D. Comparison of Topological Properties between End-Linked and Statistically Cross-Linked Polymer Networks. *J. Chem. Phys.* **2002**, *117* (13), 6300–6307.
- (21) Akagi, Y.; Gong, J. P.; Chung, U.; Sakai, T. Transition between Phantom and Affine Network Model Observed in Polymer Gels with Controlled Network Structure. *Macromolecules* **2013**, *46* (3), 1035–1040.
- (22) Arora, A.; Lin, T. S.; Beech, H. K.; Mochigase, H.; Wang, R.; Olsen, B. D. Fracture of Polymer Networks Containing Topological Defects. *Macromolecules* **2020**, *53* (17), 7346–7355.
- (23) Zhong, M.; Wang, R.; Kawamoto, K.; Olsen, B. D.; Johnson, J. A. Quantifying the Impact of Molecular Defects on Polymer Network Elasticity. *Science* **2016**, *353* (6305), 1264–1268.
- (24) Kim, J.; Zhang, G.; Shi, M.; Suo, Z. Fracture, Fatigue, and Friction of Polymers in Which Entanglements Greatly Outnumber Cross-Links. *Science* **2021**, *374* (6564), 212–216.
- (25) Griffith, A. A. The Phenomena of Rupture and Flow in Solids. *Philos. Trans. Ser. A* **1920**, *221*, 163–168.
- (26) Thomson, R.; Hsieh, C.; Rana, V. Lattice Trapping of Fracture Cracks. *J. Appl. Phys.* **1971**, *42* (8), 3154–3160.
- (27) Curtin, W. A. On Lattice Trapping of Cracks. *J. Mater. Res.* **1990**, *5* (7), 1549–1560.
- (28) Marder, M. Effects of Atoms on Brittle Fracture. *Int. J. Fract.* **2004**, *130* (2), 517–555.
- (29) Wang, S.; Hu, Y.; Kouznetsova, T. B.; Sapir, L.; Chen, D.; Herzog-Arbeitman, A.; Johnson, J. A.; Rubinstein, M.; Craig, S. L. Facile Mechanochemical Cycloreversion of Polymer Cross-Linkers Enhances Tear Resistance. *Science* **2023**, *380* (6651), 1248–1252.
- (30) Beech, H. K.; Wang, S.; Sen, D.; Rota, D.; Kouznetsova, T. B.; Arora, A.; Rubinstein, M.; Craig, S. L.; Olsen, B. D. Reactivity-Guided Depercolation Processes Determine Fracture Behavior in End-Linked Polymer Networks. *ACS Macro Lett.* **2023**, *12*, 1685–1691.
- (31) Sakai, T.; Matsunaga, T.; Yamamoto, Y.; Ito, C.; Yoshida, R.; Suzuki, S.; Sasaki, N.; Shibayama, M.; Chung, U. II. Design and Fabrication of a High-Strength Hydrogel with Ideally Homogeneous Network Structure from Tetrahedron-like Macromonomers. *Macromolecules* **2008**, *41* (14), 5379–5384.

(32) Zhukhovitskiy, A. V.; Zhong, M.; Keeler, E. G.; Michaelis, V. K.; Sun, J. E.; Hore, M. J.; Pochan, D. J.; Griffin, R. G.; Willard, A. P.; Johnson, J. A. Highly Branched and Loop-Rich Gels via Formation of Metal-Organic Cages Linked by Polymers. *Nat. Chem.* **2016**, *8* (1), 33–41.

(33) Hartquist, C. M.; Lin, S.; Zhang, J. H.; Wang, S.; Rubinstein, M.; Zhao, X. An Elastomer with Ultrahigh Strain-Induced Crystallization. *Sci. Adv.* **2023**, DOI: [10.1126/sciadv.adj0411](https://doi.org/10.1126/sciadv.adj0411).